An Improved Dynamics Modeling During Milling of the Thin-walled Parts Based on Magnetorheological Damping Fixture

Xiaohui Jiang (jiangxh@usst.edu.cn)
University of Shanghai for Science and Technology
Ning Yang
University of Shanghai for Science and Technology
Yong Zhang
University of Shanghai for Science and Technology
Shan Gao
2. Shanghai Aircraft Manufacturing Company Limited

Research Article

Keywords: thin-walled part, vibration suppression, dynamic response, magnetorheological damping fixture, milling

Posted Date: May 5th, 2021

DOI: https://doi.org/10.21203/rs.3.rs-488392/v1

An Improved Dynamics Modeling During Milling of the Thin-walled Parts Based on Magnetorheological Damping Fixture

Xiaohui Jiang[1], Ning Yang[1], Yong Zhang[1], Shan Gao[2]

1. College of Mechanical Engineering, University of Shanghai for Science and Technology, Shanghai 200093, China

2. Shanghai Aircraft Manufacturing Company Limited, China

Abstract: Aerospace thin-walled parts vibrates during the process of milling due to their characteristics of low rigidity, which influences the machining quality of the workpiece. Based on the characteristics of magnetorheological fluid excitation solidification, a magnetorheological damping fixture is designed to semi-actively suppress the vibration generated during the machining process. This paper simplifies the multi-characteristic structure of aerospace thin-walled parts into rectangular thin plates. In accordance with Kirchhoff G.'s small deflection bending theory of elastic thin-plates and Daramberg's principle, the differential equations for the transverse vibration of the thin-walled parts are established, which aims to obtain the natural frequency as well as vibration mode function of the thin-walled parts. In consideration of damping characteristics and the external dynamic milling force after the magnetorheological fluid excitation solidification, this paper uses the mode superposition method and an improved dynamic response mathematical model of the magnetorheological damping fixture thin-walled parts system of the linear multiple degrees of freedom, which has different volumes of magnetorheological fluids under forced vibration, was established. The maximum error between the predicted and measured values of the fixture-workpiece system dynamic response of displacement and acceleration is 16.2% and 15.5%, respectively. Finally, this paper verifies the feasibility as well as the effectiveness of the model through dynamics experiment and milling machining experiment.

Keywords: thin-walled part, vibration suppression, dynamic response, magnetorheological damping fixture, milling

1 Introduction

The thin-walled parts, due to the light weight and high strength, is widely used in aerospace. However, machining vibration, cutting force heat, and local stiffness reduction cause poor machining quality of thin-walled parts. Currently, a great number of studies have been carried out on traditional clamping strategies [1-3], but there are few studies on the use of new magnetorheological fixtures to clamp thin-walled parts to suppress milling vibration.

Currently, people have done a great number of studies on the optimization of clamping constraints for thin-walled workpieces. The fixture layout optimization is aimed at making the deformation or vibration of the fixture smaller and optimizing the positioning layout reasonably. It is mainly divided into two categories. One is on the basis of vibration reduction requirements to ensure that the layout plan can constrain the freedom of the workpiece and ensure its stability; the other one is based on the minimum deformation positioning layout so as to ensure that the positioning point is optimized when the positioning is perfect, thereby making the overall plastic

*Dr. Xiaohui Jiang
University of Shanghai for Science & Technology, Shanghai 200093 China.
Tel: +86 15121029145, E-mail: jiangxh@usst.edu.cn

deformation decrease. Selvakumar et al. [4] presented an optimal fixture design algorithm based on artificial neural network and carried out experimental design. In order to reduce the maximum elastic deformation of the workpiece in the process of processing, the layout scheme of the workpiece was designed. Armillott et al. [5] judged the correctness of the workpiece position through judging whether the rank of the position matrix determinant was equal to the number of singular values of the position matrix. Zheng et al. [6] established a fixture mathematical model on the basis of shape closure and force closure, who developed an algorithm which could accurately select fixture positioning points. Wan et al. [7] optimized the fixture layout on the basis of a novel nonlinear programming problem of frequency sensitivity, and maximized the natural frequency of the fixture-workpiece system. To sum up, the research on clamping constraints of thin-walled parts mainly introduces the finite element methods as well as the intelligent algorithms. The research gradually shifts from static modeling to dynamic modeling. However, these work only focus on fixture layout optimization, making fixture-workpiece system vibration become smaller. There is no research on increasing the system damping to suppress the vibration.

In terms of fixture-workpiece system dynamics modeling and process stability analysis, Seguy et al. [8] combined the finite element method as well as the excitation test. They used the multi-modal method to establish a thin-walled milling machining model. Meshreki et al. [9] used a semi-analytical method to study the impact of workpiece wall thickness changes on the dynamics of the process system for the processing of panel and frame parts. Li et al. [10] put forward a nonlinear dynamics model for milling titanium alloy thin-walled parts in consideration of process damping. They designed an anti-vibration clearance angle to suppress chatter based on this model. Zhou et al. [11] proposed an optimal selection method of cutting parameters based on single-line toolpath to suppress cutting chatter aiming at the issue of toolpath dependent machining vibration in multi-axis milling of hollow fan blades. Liu et al. [12] applied the Hermite difference and put forward an efficient full-discrete method (HFDM) for dealing with the stability of the milling process. Lv et al. [13] put forward a complete discretization method (RKCDM) based on Runge-Kutta. A set of time period coefficients and delay differential equations (DDE) were used for describing the delay of change to predict the milling stability with the change of spindle speed. Luo et al. [14] optimized the machining allowance distribution and material removal order in accordance with the machining vibration diagram. Such optimization improved the stability of the machining process and reduced the deformation of the workpiece. Wan et al. [15] put forward an assessment method on the impact of fixture layout on the dynamic response of the machining process for the milling process of frame-like thin-walled parts. Zeng et al. [16] established a tool-fixture-workpiece system model for the vibration problem during the processing of flexible components, and optimized the layout of the fixture design, which could effectively suppress vibration and predict vibration displacement response. As for the fact that the existing point contact model can't accurately describe the dynamic behavior of the fixture-complex surface workpiece system any longer, Wang et al. [17] put forward a dynamic modeling method based on finite element for fixtures and turbine blades. They also predicted deformation and workpiece displacement errors. Meshreki et al. [18] established a fixture-workpiece system dynamic model on the basis of the power spectrum method for the milling process of aerospace thin-walled frame parts so as to describe the interaction as well as dynamic response between the workpiece, fixture and cutting force. Dong et al. [19] adopted a virtual spring-damper model to describe the contact between the positioning element and the workpiece. They analyzed and predicted the static deformation resulted from the clamping force and the dynamic deformation

resulted from the milling force on the basis of the finite element method. Rai et al. [20] made use of a combination of finite element and mathematical modeling to simulate the offset, elastoplastic deformation, cutting stress and instantaneous cutting temperature of complex frame-like structural parts during the milling process. The common point of the studies mentioned above is that the fixture system belongs to the passive mode, but there has been no research on semi-active vibration abatement methods so far.

The semi-active vibration abatement method can quickly change the stiffness and dynamic damping of the system through a small amount of energy input, thereby improving processing stability. Yang et al. [21] put forward a thin-walled workpiece vibration abatement device in accordance with the principle of electromagnetic induction, which could use the generated damping force for suppressing vibration. Pour et al. [22] introduced an integrated mechatronic model for the chatter analysis of a machine tool equipped with MR damper, and the stiffness and damping of the machine tool are varied semi-actively by means of a magnetorheological (MR) damper to suppress chatter. Yang et al. [23] proposed a lightweight damping device with utilizing eddy current damping, and it can be easily attached onto the workpiece surface by glue. There is a great amount of concentrated force produced by the traditional control structure, but the force produced by magnetorheological fluids is relatively uniform. Ma et al. [24, 25] designed magnetorheological fixtures and used the lagrangian method to establish a fixture-workpiece system dynamic equation in consideration of external damping factors, thereby evaluating the stability of the milling process under damping control. Bae et al. [26] developed a magnetically tuned mass damper (mTMD) to suppress the vibration of a cantilever panel similar to satellite solar panels. Xin et al. [27] put forward a shear valve mode MRF damper for pipeline vibration control. They made use of a linear quadratic regulator to study the optimal damping force of the MRF damper, and establishing a dynamic model and equation of state for the pipeline. The above research work didn't take the impact of magnetorheological fluid volumes change on the damping characteristics of the fixture-workpiece system into account and it didn't simplify the thin-walled parts into a more reasonable rectangular thin plate model either. However, the study is the dynamic response of forced vibration under magnetorheological damping.

The organization of this paper is as follows: The second section simplified aerospace thin-walled parts into rectangular thin plates. In accordance with Kirchhoff G.'s small deflection bending theory of elastic thin-plates and Daramberg's principle and mode superposition principle, the natural frequency and main mode of vibration were calculated, and the dynamic response mathematical model of the magnetorheological damping fixture thin-walled parts system under forced vibration was established so as to evaluate the stability of the fixture-workpiece system. Based on this model, the dynamics experiments of aerospace thin-walled parts and the milling experiments of annular thin-walled parts were designed. The third section discussed and analyzed the experimental results and the machining quality so as to verify the feasibility and effectiveness of the model. The fourth section drew a conclusion of the full paper.

2. Methodology

This paper has developed a magnetorheological damping fixture. Under the action of a magnetic field, the ferromagnetic particles of the magnetorheological fluid in the fixture are rapidly magnetized along the direction of the magnetic field, which gather to form a magnetic chain structure and adhere closely to the surface of the workpiece. As shown in Fig. 1. It is solidified by Newtonian fluid into a solid state. Magnetorheological fluid can be used to fill a variety of irregular

thin-walled parts. It can play the part of multi-point auxiliary support. Besides, the magnetorheological fluid solidifies and generates shear stress to clamp thin-walled parts. When milling on a machine tool, it provides a damping force to offset the milling force, which can increase the rigidity of the workpiece and suppress the machining vibration. When the magnetic field disappears, the magnetorheological fluid is inverted into a liquid, and the clamping is both quick and convenient. This paper studied the effect of restraining flutter of magnetorheological fixture through the theory of semi-active vibration control.

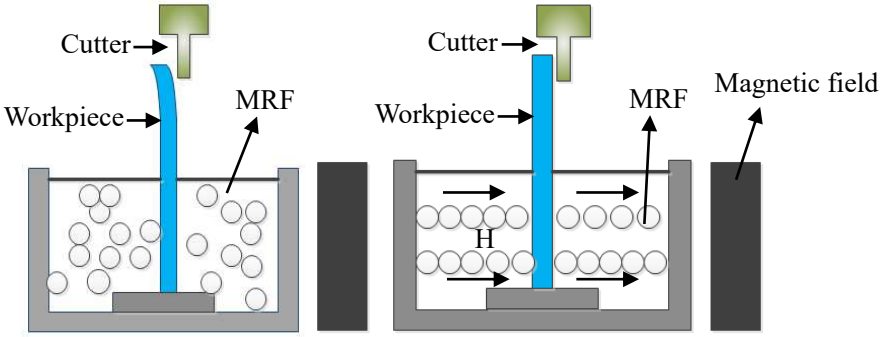

Fig. 1 The magnetorheological fluid in the magnetorheological fixture is magnetically solidified.

In the process of machining, the height of thin-walled parts is generally much smaller than the size of the bottom surface, and this forms a thin flat elastic body. Although the thin-walled parts are very thin, they still have a certain bending rigidity and the deflection is much smaller than its thickness. Thus, the thin-walled parts are simplified to a more reasonable rectangular thin plate. The study on its dynamic response during milling can provide methods and strategies for suppressing vibration.

2.1 Natural frequency and main vibration mode of thin-walled parts

The Aerospace thin-walled parts that were used in the experiment are shown in Fig. 2. There are upper and lower ends, and there are many grooves on the side. The thinnest part of the wall is only 1*mm*. This paper simplified the model as a rectangular thin-walled plate of equal thickness with length a, width b, thickness h, and density ρ, as shown in Fig. 3, which replaced the micro-element body $hdxdy$ with any rectangular micro-element body $dxdy$ on the neutral surface and expressed the load and the internal force on the cross section on the neutral plane, as shown in Fig. 4. In Fig. 4, Q_x, Q_y, Q_z are the transverse shear forces per unit width, and M_x, M_y, M_z are the upward bending per unit width bending moment, M_{xy}, M_{yx}, M_{yz}, M_{zy} are the torque per unit width, the exciting force distributed on the unit area is $p(x,y,t)$, the inertial force per unit area of the thin plate is $-\rho h\frac{\partial^2 w}{\partial t^2}$, w is the deformation deflection of the rectangular thin plate. In accordance with Kirchhoff G.'s small deflection bending theory of elastic thin-plates and Daramberg's principle, the differential equation for the transverse vibration of the thin plate is established as follows:

$$D_0\nabla^4 w+\rho h\frac{\partial^2 w}{\partial t^2}=p(x,y,t) \tag{1}$$

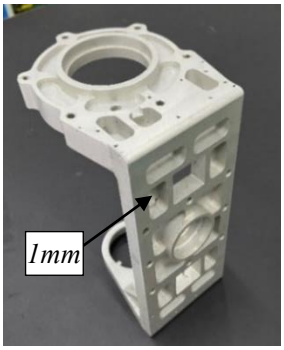

Fig. 2 Aerospace thin-walled parts

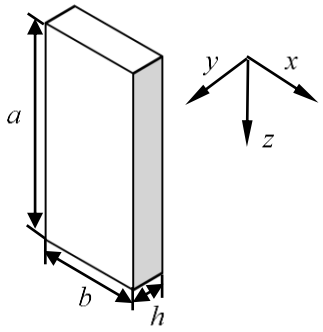

Fig. 3 Simplified rectangular thin-walled plate

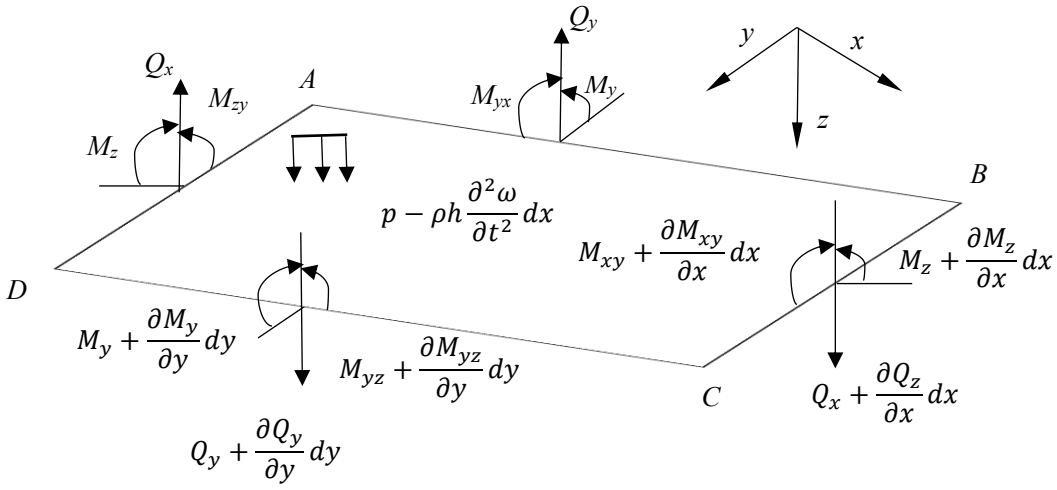

Fig. 4 The rectangular micro-element body on the neutral surface of the rectangular thin-walled plate

In the formula, $D_0=\frac{Eh^3}{12(1-\mu^2)}$ is the bending stiffness of the thin plate, E is the elastic modulus of the thin plate, μ is the Poisson's ratio, and ∇^4 is the reharmonization operator, $\nabla^4=\frac{\partial^4}{\partial x^4}+2\frac{\partial^4 w}{\partial x^2\partial y^2}+\frac{\partial^4}{\partial y^4}$.

In the differential equation of the lateral bending vibration of the thin plate, set the excitation force $p(x,y,t)=0$, then the differential equation of the free vibration of the thin plate can be obtained as follows:

$$\nabla^4 w+\frac{\rho h}{D_0}\frac{\partial^2 w}{\partial t^2}=0 \tag{2}$$

Using the semi-inverse solution method, it is assumed that the free vibration displacement response of the thin plate is as follows:

$$w(x,y,t)=W(x,y)\sin(\omega t+\varphi) \tag{3}$$

In the formula, $W(x, y)$ is the main vibration mode of the thin plate. In accordance with the boundary conditions, the following formula can be obtained:

$$\nabla^4 W-\beta^4 W=0 \tag{4}$$

In the formula,

$$\beta^4=\frac{\rho h}{D_0}\omega^2 \tag{5}$$

The main mode of Euler Bernoulli beam is $C_i sin\frac{i\pi x}{l}$, (i=1, 2, …). In accordance with this formula, the main mode of rectangular thin plate can be assumed as follows:

$$W_{i,j}(x,y)=A_{i,j}\sin\frac{i\pi x}{a}\sin\frac{j\pi y}{b} \tag{6}$$

In the formula, A_{ij} are related to the initial conditions. Through substituting formula (5) into formula (4), the following can be obtained:

$$\left\{\left[\left(\frac{i\pi}{a}\right)^2+\left(\frac{j\pi}{a}\right)^2\right]^2-\beta^4\right\}A_{i,j}\sin\frac{i\pi x}{a}\sin\frac{j\pi y}{b}=0 \tag{7}$$

In order to make this condition meet all points on the neutral surface of the rectangular thin plate, that is, both x and y can be met, so the frequency equation must meet the following relationship:

$$\left[\left(\frac{i\pi}{a}\right)^2+\left(\frac{j\pi}{a}\right)^2\right]^2-\beta^4=0 \tag{8}$$

Through substituting equation (5) into equation (8), the natural frequencies of each order of the rectangular thin plate can be solved as follows:

$$\omega_{i,j}=\pi^2\left(\frac{i^2}{a^2}+\frac{j^2}{b^2}\right)\sqrt{\frac{D_0}{\rho h}}\qquad i=1,2,\cdots\quad j=1,2\cdots \tag{9}$$

2.2 Dynamic response of magnetorheological damping fixture thin-walled parts system with different volumes of magnetorheological fluids under forced vibration

Magnetorheological fluid damping effect: Under the action of a magnetic field, the ferromagnetic particles in the magnetorheological fluid are magnetized and aggregated into a chain-like particle molecular structure under the action of the magnetic field. When the system is in an excitation state, the magnetic chain generates dislocation motion. Internal molecular friction dissipates the energy input to the system. Thus, the damping produced by the magnetorheological fluid after solidification by the magnetic field is regarded as structural damping. However, in order to facilitate vibration analysis, linear equivalent viscous damping is used for approximate calculation.

When the energy is consumed in one cycle of equivalent viscous damping and magnetorheological structure damping under the action of simple harmonic excitation force， it can be shown as follows respectively:

$$\Delta E=\pi c_e B^2\omega \tag{10}$$

$$\square W=\varphi V B^2 \tag{11}$$

In the formula, B is the amplitude, φ is a constant related to the type and volume fraction of ferromagnetic particles in the magnetorheological fluid, and V is the volume of the magnetorheological fluid. Through substituting formula (11) into (10) to make the energy consumed by the two damping in one cycle be the same, the linear equivalent damping coefficient can be obtained as follows:

$$c_e = \frac{\varphi V}{\pi \omega} \tag{12}$$

The differential equation for forced vibration of a linear multi-degree-of-freedom thin-walled part with magnetorheological damping is:

$$D_0 \nabla^4 w + c_e \nabla^2 \frac{\partial w}{\partial t} + \rho h \frac{\partial^2 w}{\partial t^2} = F(x, y, t) \tag{13}$$

In the formula, ∇^2 is harmonic operator, $\nabla^2 = \frac{\partial^2}{\partial x^2} + \frac{\partial^2}{\partial y^2}$, $F(x, y, t)$ is generalized milling force.

Through using the mode superposition method to solve the equation (9) and using the regular mode $\psi_{i,j}(x, y)$ to transform the vibration deflection response $w(x, y, t)$ of the thin plate, the following formulation can be obtained:

$$w(x, y, t) = \sum_{i=1}^{\infty} \sum_{j=1}^{\infty} \psi_{i,j}(x, y) \eta_{i,j}(t) \tag{14}$$

In the formula, $\eta_{i,j}(t)$ is the canonical coordinate. Through substituting formula (14) into the vibration differential equation (13), the following formulation can be obtained:

$$D_0 \sum_{i=1}^{\infty} \sum_{j=1}^{\infty} \eta_{i,j}(t) \iint_{\Omega} \left(\nabla^4 \psi_{i,j} \right) + c_e \sum_{i=1}^{\infty} \sum_{j=1}^{\infty} \left(\nabla^2 \psi_{i,j} \right) \dot{\eta}_{i,j}(t) + \rho h \sum_{i=1}^{\infty} \sum_{j=1}^{\infty} \psi_{i,j} \ddot{\eta}_{i,j}(t) = F(x, y, t) \tag{15}$$

By multiplying both sides of the above equation by another regular mode shape $\psi_{r,s}(x, y)$ and integrating x and y on the area domain Ω of the rectangular thin plate, the following formulation can be obtained:

$$\sum_{i=1}^{\infty} \sum_{j=1}^{\infty} \eta_{i,j}(t) \iint_{\Omega} D_0 \left(\nabla^4 \psi_{i,j} \right) \psi_{r,s} dxdy + \sum_{i=1}^{\infty} \sum_{j=1}^{\infty} \dot{\eta}_{i,j}(t) \iint_{\Omega} c_e \left(\nabla^2 \psi_{i,j} \right) \psi_{r,s} dxdy + \sum_{i=1}^{\infty} \sum_{j=1}^{\infty} \ddot{\eta}_{i,j}(t) \iint_{\Omega} \rho h \psi_{i,j} \psi_{r,s} dxdy = \iint_{\Omega} F(x, y, t) \psi_{r,s} dxdy \tag{16}$$

In accordance with the orthogonalization of the canonical mode, the vibration equation under the decoupled canonical coordinates is shown as follows:

$$\ddot{\eta}_{r,s}(t) + 2\xi_{r,s} \omega_{r,s} \dot{\eta}_{r,s}(t) + \omega_{r,s}^2 \eta_{r,s}(t) = q_{r,s}(t) \tag{17}$$

In the formula, $q_{r,s(t)}$ is the regular milling force, and $q_{r,s}(t) = \iint_{\Omega} F(x, y, t) \psi_{r,s} dxdy$.

Assume that the initial conditions of the magnetorheological damping thin plate system are as follows:

$$w(x, y, t) = g_1(x, y), \frac{\partial w}{\partial t}|_{t=0} = g_2(x, t) \tag{18}$$

Substituting formula (18) into formula (14), the following formulation can be obtained:

$$w(x, y, 0) = g_1(x, y) = \sum_{i=1}^{\infty} \sum_{j=1}^{\infty} \psi_{i,j}(x, y) \eta_{i,j}(0) \tag{19}$$

$$\frac{\partial w}{\partial t}|_{t=0} = g_2(x, y) = \sum_{i=1}^{\infty} \sum_{j=1}^{\infty} \psi_{i,j}(x, y) \dot{\eta}_{i,j}(0) \tag{20}$$

Through multiplying both sides of the above two equations by $\rho h \psi_{r,s}(x, y)$ and integrating them on the area Ω of the thin plate, and using the orthogonalization condition of the canonical mode, the initial conditions of the canonical coordinates can be obtained as follows:

$$\eta_{r,s}(0) = \iint_{\Omega} \rho h g_1(x, y) \psi_{r,s}(x, y) dxdy \tag{21}$$

$$\dot{\eta}_{r,s}(0) = \iint_{\Omega} \rho h g_2(x, y) \psi_{r,s}(x, y) dxdy \tag{22}$$

In accordance with the principle of mode superposition, the forced vibration response of a multi-degree-of-freedom thin-walled workpiece system constrained by magnetorheological damping can be considered as the result of the superposition of multiple single-degree-of-freedom vibration responses. In accordance with Duhamel's integral, the response of the system to any excitation force can be considered as the sum of the response to a series of impulses in the corresponding time interval, and the regular response of the system can be obtained from equations (17), (21) and (22) as follows:

$$\eta_{r,s}(t)=e^{-\xi_{r,s}\omega_{r,s}t}\left[\eta_{r,s}(0)\cos\omega'_{r,s}t+\frac{\dot{\eta}_{r,s}(0)+\xi_{r,s}\omega_{r,s}\eta_{r,s}(0)}{\omega'_{r,s}}\sin\omega'_{r,s}t\right]+\frac{1}{\omega'_{r,s}}\int_0^t q_{r,s}(\tau)e^{-\xi_{r,s}\omega_{r,s}(t-\tau)}\sin\omega'_{r,s}(t-\tau)d\tau \tag{23}$$

In the formula, $\omega'_{r,s}$, $\xi_{r,s}$ are the natural frequency and damping ratio of the magnetorheological damped thin-walled parts system, $\omega'_{r,s}=\sqrt{1-\xi_{r,s}^2}\,\omega_{r,s}$, $\xi_{r,s}=\dfrac{c_e}{2abh\rho\omega_{r,s}}$.

Through the normalized condition, convert the main mode of vibration $W_{i,j}(x,y)$ to the regular mode of vibration $\psi_{i,j}(x,y)$:

$$\iint_\Omega \rho h W_{i,j}^2(x,y)dxdy=\int_0^a\int_0^b \rho h\left(A_{i,j}\sin\frac{i\pi x}{a}\sin\frac{j\pi y}{b}\right)^2 dxdy=1 \tag{24}$$

The solution is $A_{i,j}=\sqrt{\dfrac{4}{abh\rho}}$, so the regular mode shape can be solved as:

$$\psi_{i,j}(x,y)=\sqrt{\frac{4}{abh\rho}}\sin\frac{i\pi x}{a}\sin\frac{j\pi y}{b} \tag{25}$$

Through substituting formula (25) and formula (23) into formula (14), the displacement response of forced vibration of the magnetorheological damping fixture thin-walled parts system related to the magnetorheological fluid volumes under generalized coordinates can be obtained as follows:

$$w(x,y,t)=\sqrt{\frac{4}{abh\rho}}\sin\frac{i\pi x}{a}\sin\frac{j\pi y}{b}\sum_{r=1}^{\infty}\sum_{s=1}^{\infty}e^{-\xi_{r,s}\omega_{r,s}t}\left(\eta_{r,s}(0)\cos\omega'_{r,s}t+\frac{\dot{\eta}_{r,s}(0)+\xi_{r,s}\omega_{r,s}\eta_{r,s}(0)}{\omega'_{r,s}}\sin\omega'_{r,s}t\right)+\frac{1}{\omega'_{r,s}}\int_0^t q_{r,s}(\tau)e^{-\xi_{r,s}\omega_{r,s}(t-\tau)}\sin\omega'_{r,s}(t-\tau)d\tau \tag{26}$$

The second-order derivative of the displacement response in formula (26) can be used to obtain the acceleration response:

$$\begin{aligned}A(x,y,t)=\ddot{w}(x,y,t)=\sum_{r=1}^{\infty}\sum_{s=1}^{\infty}\sqrt{\frac{4}{abh\rho}}\sin\frac{i\pi x}{a}\sin\frac{j\pi y}{b}\Bigg\{&\xi_{r,s}^2\omega_{r,s}^2\left[e^{-\xi_{r,s}\omega_{r,s}t}\left(\eta_{r,s}(0)\cos\omega'_{r,s}t+\frac{\dot{\eta}_{r,s}(0)+\xi_{r,s}\omega_{r,s}\eta_{r,s}(0)}{\omega'_{r,s}}\sin\omega'_{r,s}t\right)+\frac{1}{\omega'_{r,s}}\int_0^t q_{r,s}(\tau)e^{-\xi_{r,s}\omega_{r,s}(t-\tau)}\sin\omega'_{r,s}(t-\tau)d\tau\right]\\&-\xi_{r,s}\omega_{r,s}e^{-\xi_{r,s}\omega_{r,s}t}\left(-\omega'_{r,s}\eta_{r,s}(0)\sin\omega'_{r,s}t+\dot{\eta}_{r,s}(0)\cos\omega'_{r,s}t+\xi_{r,s}\omega_{r,s}\eta_{r,s}(0)\cos\omega'_{r,s}t\right)\\&+e^{-\xi_{r,s}\omega_{r,s}t}\left(-\omega'^{\,2}_{r,s}\eta_{r,s}(0)\cos\omega'_{r,s}t-\omega'_{r,s}\dot{\eta}_{r,s}(0)\sin\omega'_{r,s}t-\xi_{r,s}\omega_{r,s}\omega'_{r,s}\eta_{r,s}(0)\sin\omega'_{r,s}t\right)\\&+\frac{q_{r,s}(t)}{\omega'_{r,s}}\left[\xi_{r,s}\omega_{r,s}e^{-\xi_{r,s}\omega_{r,s}t}\left(-\xi_{r,s}\omega_{r,s}\sin\omega'_{r,s}t+\omega'_{r,s}\cos\omega'_{r,s}t\right)\int_0^t q_{r,s}(\tau)e^{\xi_{r,s}\omega_{r,s}\tau}\cos\omega'_{r,s}\tau d\tau\right]\\&-\frac{q_{r,s}(t)}{\omega'_{r,s}}\left[\xi_{r,s}\omega_{r,s}e^{-\xi_{r,s}\omega_{r,s}t}\left(\xi_{r,s}\omega_{r,s}\cos\omega'_{r,s}t+\omega'_{r,s}\sin\omega'_{r,s}t\right)\int_0^t q_{r,s}(\tau)e^{\xi_{r,s}\omega_{r,s}\tau}\sin\omega'_{r,s}\tau d\tau\right]\Bigg\}\end{aligned} \tag{27}$$

2.3 Dynamics experiment setup for aerospace thin-walled parts

In order to verify the validity of the model and analyze the influence of different magnetorheological fluid volumes on the stiffness and damping characteristics of the fixture workpiece system, the relevant dynamics experiments are designed in this paper. As shown in Fig.

5, when fixing the aerospace thin-walled parts in the magnetorheological damping fixture and adding 0L, 3L, 5L, 7L magnetorheological fluids into the fixture box respectively, the 7L magnetorheological fluid can basically reach the state of fully covering the thin-walled parts. As shown in Fig. 6, the modal hammer percussion experiment uses a laser vibrometer (PSV-400) to test the dynamic response of adding different volumes of magnetorheological fluid and analyzes the impact of magnetorheological fluid volumes change on suppressing flutter of magnetorheological damping fixture.

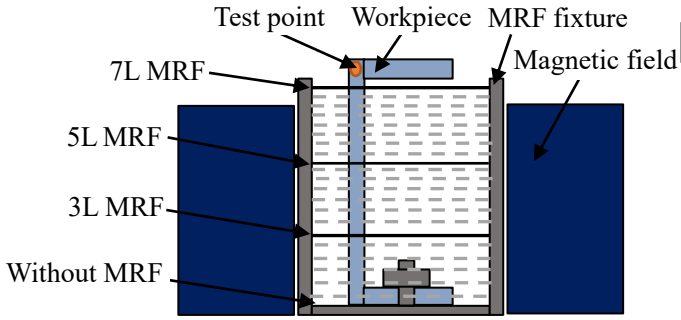

Fig. 5 Fixtures with different volumes of magnetorheological fluid

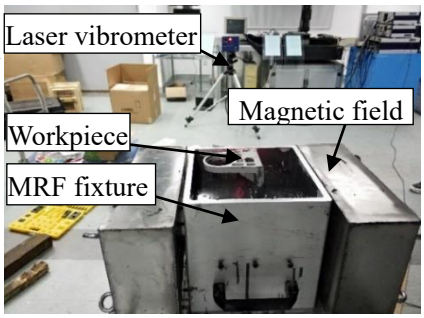

Fig. 6 Modal percussion experiment

2.4 Experiment setup for milling of annular thin-walled parts

In order to verify the impact of the magnetorheological damping fixture filled with different volumes of magnetorheological fluid on the processing of different types of thin-walled parts, a magnetorheological damping composite fixture for clamping annular thin-walled parts was designed to study the change of milling force and milling vibration acceleration . As shown in Fig. 7, for the existing annular aluminum alloy blanks, the inner wall is reamed from 26mm to 27*mm*, and the thinnest wall thickness is 1.5*mm*. As shown in Fig. 8, by adding 0.1L, 0.2L, 0.3L magnetorheological fluid to the magnetorheological damping fixture and installing a dynamometer (Kistler, 9139AA) at the bottom of the fixture, the milling force can be measured. Beside it is possible to choose ∅4*mm*4-edge cemented carbide milling cutter, the process parameters are spindle speed 12000 *r/min*, cutting depth 1 *mm*, feed rate 100 *mm/min*, and milling on a three-axis milling machine (Carver S600).

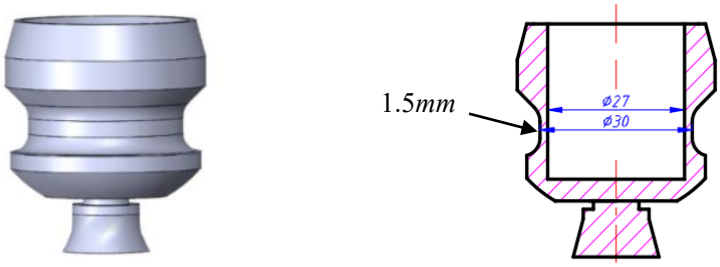

(a) Three-dimensional drawing of annular thin-walled parts (b) The dimensions of annular thin-walled part

Fig. 7 Schematic diagram of ring-shaped thin-walled parts

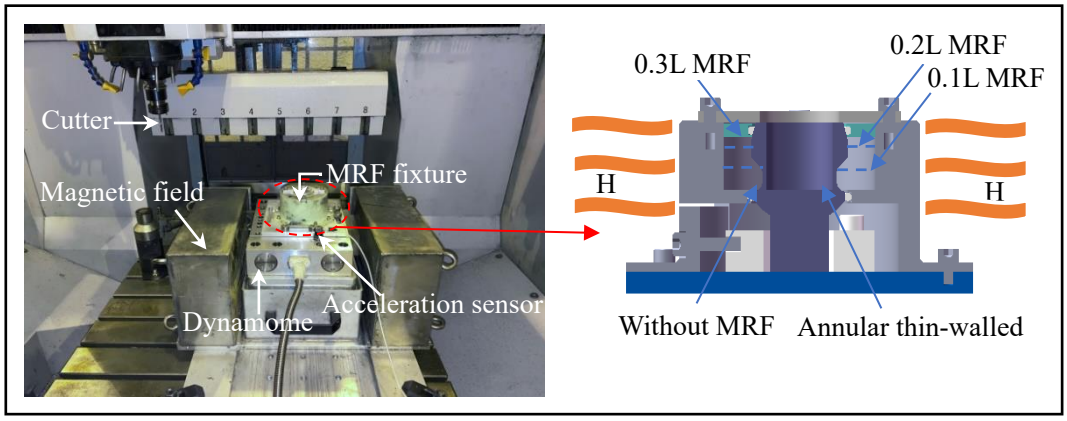

Fig. 8 Measurement of milling force and vibration acceleration

3. Results and discussion

This section mainly verifies the dynamic model that is proposed in the previous section. It also analyzes the impact of different magnetorheological fluid volumes on the stiffness and damping characteristics of the fixture-workpiece system. Besides, it studies the milling characteristics of different magnetorheological fluid volumes, including the impact of milling force and milling vibration acceleration. And it also discusses the processing quality of thin-walled parts after milling.

3.1 Verification of dynamic model of the magnetorheological damping fixture-workpiece system

In order to accurately analyze the difference in the dynamic characteristics of the magnetorheological damping fixture-workpiece system resulted from the change of the magnetorheological fluid volume, the dynamics experiment results of aerospace thin-walled parts were discussed.。 Fig. 9 plots the frequency response function of the fixture-workpiece system. The results has shown that, except for the addition of 7L magnetorheological fluid, in the first-order mode, the amplitude of the frequency response function is greatly reduced with the increase of the volume of the added magnetorheological fluid and the natural frequency gradually increases; the natural frequency value of the system is the smallest when no magnetorheological fluid is added, which is 441.5Hz, and the natural frequency when 5L of magnetorheological fluid is added is the largest, which is about 580.6 Hz, with an increase of 31.5%. When adding 7L magnetorheological fluid, because of the phenomenon of magnetic saturation, the magnetic field intensity set in this experiment cannot solidify all 7L magnetorheological fluid, and part of the magnetorheological fluid is still in the state of Newtonian fluid. Thus, the natural frequency of the system is slightly smaller than when adding 5L magnetorheological fluid. The whole experimental results have shown that the magnetorheological damping fixture improves the rigidity of the fixture-workpiece system effectively than that of the non-magnetorheological fixture. When the magnetorheological fluid excitation was not saturated, as the magnetorheological fluid volume increased, the greater the rigidity of the system , the better the vibration abatement effect.

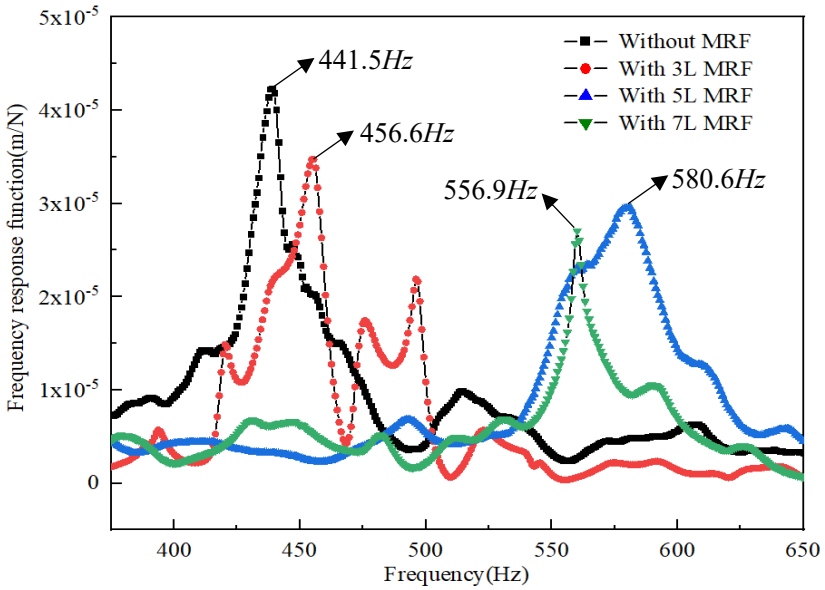

Fig. 9 The frequency response function with different magnetorheological fluid volumes added

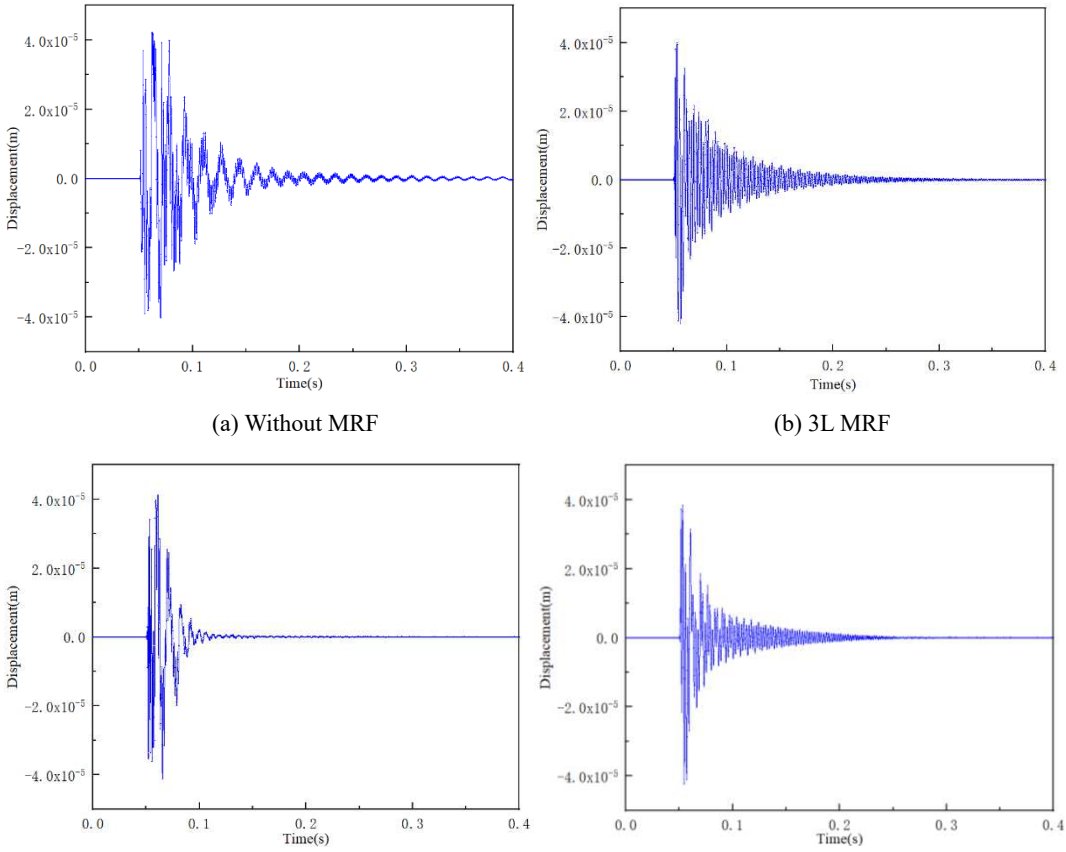

(a) Without MRF (b) 3L MRF

(c) 5L MRF (d) 7L MRF

Fig. 10 The displacement response with different magnetorheological fluid volumes added

Fig. 10 shows the displacement response of the fixture-workpiece system without magnetorheological fluid and adding different volumes of magnetorheological fluid. Table 1 shows the peak displacement and deformation corresponding to different situations and the time it takes for the vibration of the workpiece starting from excitation to the steady state. It is found that as the volume of the magnetorheological fluid added increased, the vibration deformation displacement

and the time-consuming to stabilize state gradually decreased, except for the case when 7L magnetorheological fluid was added. Since the solidified magnetorheological fluid has the damping characteristics, the energy applied to the system by external excitation was gradually dissipated through magnetorheological damping. The more magnetorheological fluid, the faster the energy dissipation, and as the system vibration tended to stabilize, it became faster. Thus, it took the longest time for the non-magnetorheological fluid fixture to stabilize, which was 0.35s, and the damping fixture with 5L magnetorheological fluid took the shortest time, which was 0.15s. The time has been decreased by 57.1%. The measured data was abnormal when 7L magnetorheological fluid was added because of the phenomenon of magnetic saturation. The entire experimental results have verified that the magnetorheological damping fixture dissipated the excitation energy faster than the non-magnetorheological fixture. When the solidification of magnetorheological fluid was in unsaturation condition, as the volumes of the magnetorheological fluid increased, the more prominent the system damping characteristics, the better the vibration abatement effect.

Table 1 Modal parameters of fixture-workpiece system with different magnetorheological fluid volumes added

MRF volume Item	Without MRF	With 3L MRF	With 5L MRF	With 7L MRF
Response maximum displacement (μm)	43.5	42.4	40.5	41.5
Excitation to Stability time-consuming (s)	0.35	0.28	0.15	0.26

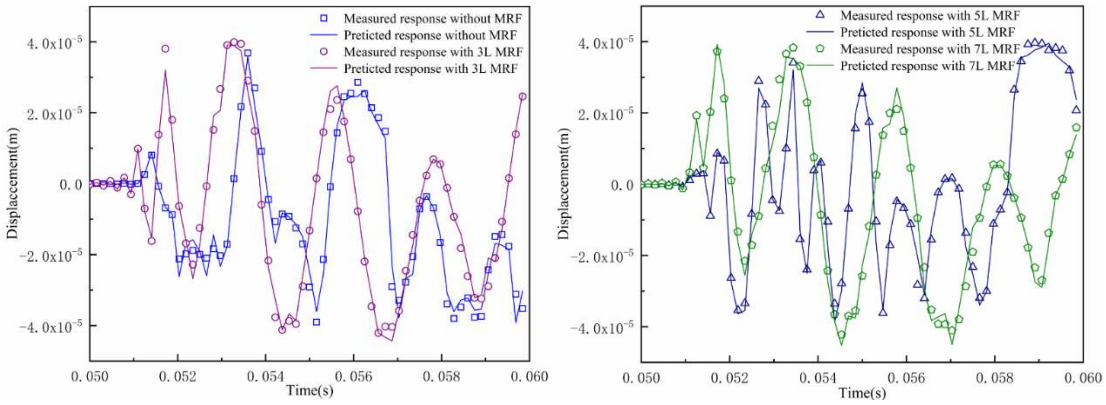

(a) Comparison of predicted and measured displacement response between without MRF and 3L MRF

(b) Comparison of predicted and measured displacement response between 5L MRF and 7L MRF

Fig. 11 Comparison of the predicted and measured displacement response with different magnetorheological fluid volumes

Fig. 11 shows the comparison of the fixture-workpiece system displacement response predictions as well as the measured values with different magnetorheological fluid volumes added. The maximum error was 16.2%. The predicted displacement response was consistent with the measured value trend. The results have verified that the dynamic model of the magnetorheological damping fixture-workpiece system could effectively predict the displacement response of the thin-walled workpieces.

3.2 Effects of the magnetorheological fluid volumes on the milling characteristics

In order to further analyze the impact of the magnetorheological damping fixture filled with

different volumes of magnetorheological fluid on the actual milling conditions, the milling force and milling vibration acceleration are discussed. They were measured in section 2.4 for the machining of annular thin-walled parts under certain milling process parameters. The measured results of the milling force experiment are shown in Fig. 12. In Fig. 12, the X direction is the tool feed direction and the Y direction is the tool width direction, so the maximum milling force in the X direction is greater than the Y direction; the Z axis is the tool spindle, which undertakes the main cutting action, so the maximum milling force in the Z direction is much larger than in the X and Y directions. As the volumes of the magnetorheological fluid in the fixture increases, the maximum milling force in the three directions gradually decreases. However, the maximum milling force in the Z-axis direction doesn't change so much. The milling force of the fixture without magnetorheological fluid is the largest. When 0.1L and 0.3L magnetorheological fluid are added, the maximum milling force in the X, Y, and Z directions of the workpiece is 52.49N, 43.56N, 58.89N, 41.38N, 31.21N, 56.16N respectively, the maximum milling force is decreased by 21.2%, 28.4%, and 4.6% respectively. The results show that the damping force provided by the solidified magnetorheological fluid can offset part of the milling force effectively. The Y direction has the best milling force control effect, followed by the X direction.

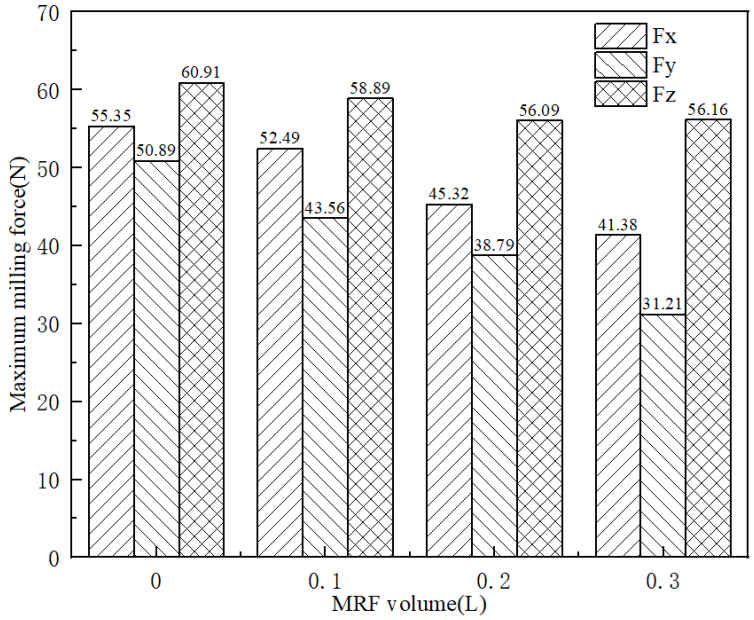

Fig. 12 The maximum milling force with different volumes of magnetorheological fluids

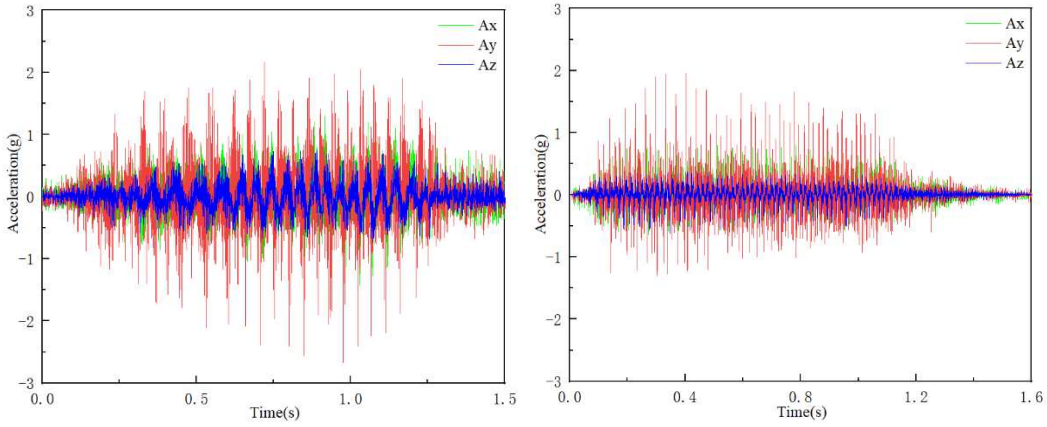

(a) Without MRF (b) 0.1L MRF

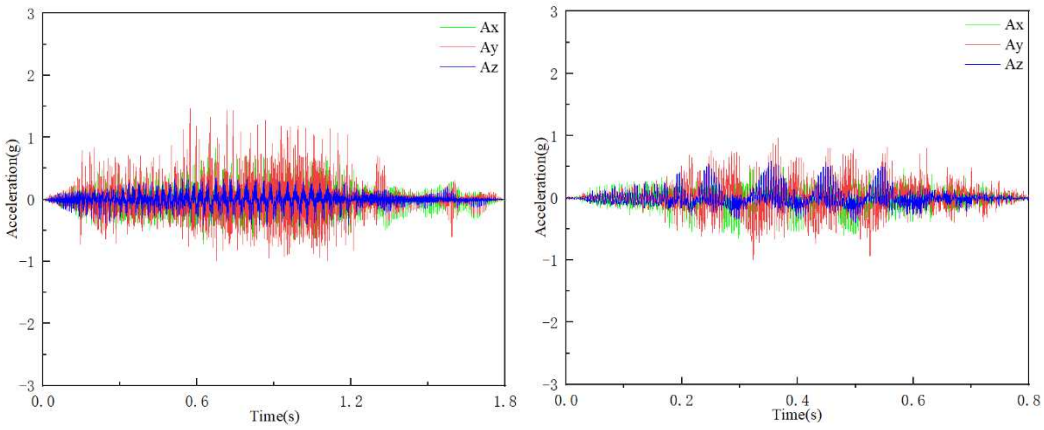

(c) 0.2L MRF (d) 0.3L MRF

Fig. 13 The milling vibration acceleration with different volumes of magnetorheological fluids

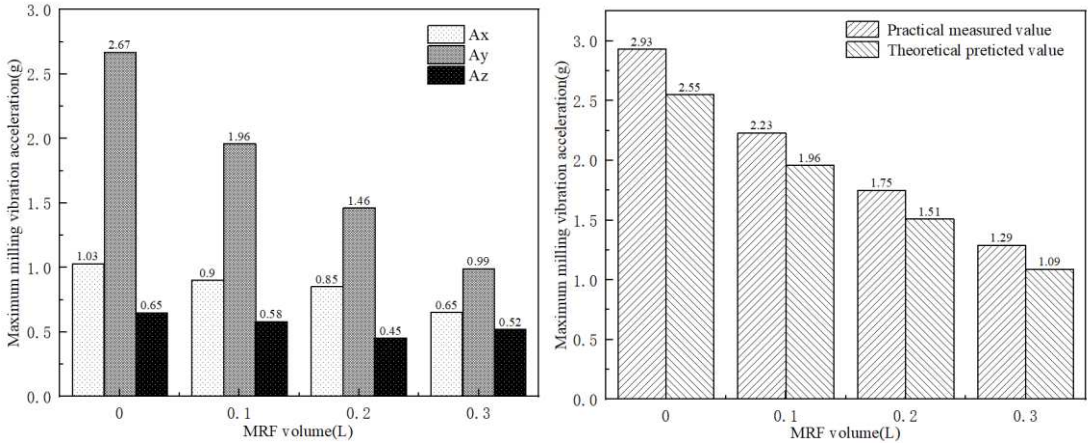

(a) Measured under different directions (b) Comparison of the predicted and measured value

Fig. 14 Maximum vibration acceleration with different volumes of magnetorheological fluids

The results of the milling vibration acceleration experiment are shown in Fig. 13 and Fig. 14(a). The milling vibration acceleration in the Z direction is the smallest, the Y direction is the largest, and the X direction follows the Y direction. With the increase in the volumes of the magnetorheological fluid in the fixture, the maximum milling vibration acceleration in each of the three directions gradually decreased. However, the maximum milling vibration acceleration in the Z-axis direction didn't change so much. The milling vibration acceleration of the fixture without magnetorheological fluid is the largest. When 0.1L and 0.3L magnetorheological fluid are added, the maximum milling vibration acceleration in the X, Y, and Z directions of the workpiece is 0.90g, 1.96g, 0.58g, 0.65g, 0.99g and 0.52g respectively. The maximum milling vibration acceleration decreases by 27.8%, 49.5%, 10.3% respectively. The results show that the magnetorheological damping fixture mainly suppresses the vibration of the workpiece in the Y direction, followed by the X direction. The milling stability of the Z direction has the least impact. This is because the Z direction is the direction of the machine tool spindle, and the rigidity is the strongest. The milling vibration has little effect in this direction, and the X direction has a constraint effect of the feeding force, so the milling vibration in the X direction is more stable than that of the Y direction. The Y direction is the tool's width cutting direction. The rigidity is the worst.

By substituting the maximum milling force measured in Fig. 13 into formula (27), the maximum milling vibration acceleration can be calculated, as shown in Fig. 14 (b). By comparing

the predicted value with the measured value, the predicted value of the maximum milling vibration acceleration is generally smaller than the measured value and the maximum error is 15.5%. This is because of the uncontrollable factors, such as external environmental vibration. The results have verified that the dynamics model of the magnetorheological damping fixture-workpiece system could effectively predict the acceleration response of the thin-walled parts under the milling force.

3.3 Effects of the magnetorheological fluid volumes on machining quality

Compared with the results of dynamic experiments and milling experiments, the processing quality of thin-walled parts can directly reflect the difference in vibration suppression of different volumes of magnetorheological fluids. This section carries out comparative analysis of vibration suppression effects according to the processing quality results in three aspects: roughness, coaxiality and cylindricity. Roughness is a significant factor for measuring the accuracy of the surface of the workpiece. It is also the standard for judging the quality of processing. This section made use of the Form Talysurfi200 surface roughness meter to test the inner surface roughness value of the milled annular thin-walled parts in the previous section. Besides, a marker was used to mark 4 points to be measured (1-4) at the same height on the surface of the inner hole (1-4). The 4 points were tested respectively and the average value was calculated. These not only reduced the error resulted from the experimental measurement, but also could judge the processing stability, as shown in Fig. 15.

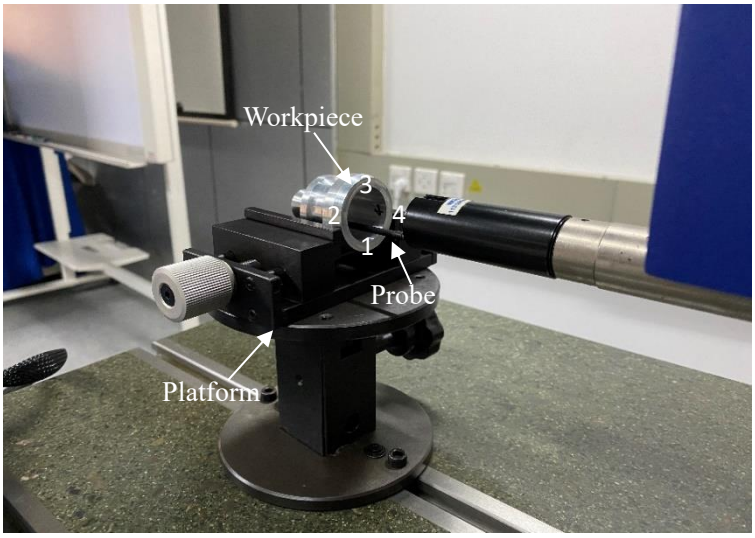

Fig. 15 Scheme of roughness measurement

In accordance with the roughness test results in Table 2, it is concluded that the use of magnetorheological damping fixtures can greatly reduce the surface roughness of the workpiece compared with non-magnetorheological fixtures. The inner hole of the workpiece is rougher after adding 0.1L and 0.3L magnetorheological fluid. The degree values Ra, Rz, and Rq are 0.25, 1.36, 0.33, 0.15, 0.83, 0.21, respectively, which are decreased by 40%, 39.0%, and 36.4% respectively.

Coaxiality theory considers the reference axis as an ideal straight line, and the measured axis bends, tilts and shifts. This section used the Talyrond 565 cylindricity meter and the PMM-C 8.10.6 ultra-high-precision three-coordinate measuring machine to test the cylindricity as well as the coaxiality of the milled workpiece. Several test points were taken on the inner surface of the workpiece so as to obtain the cylindricity as well as the position of each axis based on one of the axes, and the deviation of the two axes was compared. The field test is shown in Fig. 16.

Table 2 Results of roughness test of annular thin-walled parts

MRF volume	Test point	1	2	3	4	average value
Without MRF	Ra(μm)	0.33	0.29	0.29	0.29	0.30
	Rz(μm)	1.57	1.27	1.37	1.33	1.39
	Rq(μm)	0.49	0.38	0.38	0.37	0.41
With 0.1L MRF	Ra(μm)	0.25	0.25	0.24	0.26	0.25
	Rz(μm)	1.42	1.38	1.30	1.35	1.36
	Rq(μm)	0.35	0.31	0.33	0.32	0.33
With 0.2L MRF	Ra(μm)	0.21	0.18	0.19	0.19	0.19
	Rz(μm)	1.18	1.12	1.08	1.09	1.12
	Rq(μm)	0.25	0.27	0.26	0.21	0.25
With 0.3L MRF	Ra(μm)	0.14	0.15	0.14	0.16	0.15
	Rz(μm)	0.79	0.85	0.81	0.85	0.83
	Rq(μm)	0.19	0.20	0.19	0.25	0.21

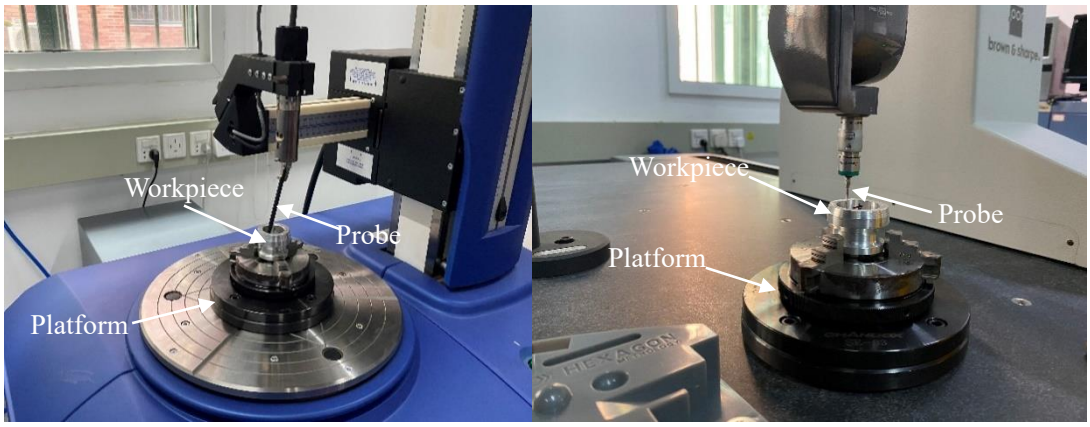

(a) Scheme of Cylindricity measurement (b) Scheme of Coaxiality measurement

Fig. 16 Scheme of cylindricity and concentricity measurement

In accordance with the test results of cylindricity and coaxiality of annular thin-walled parts in Table 3, it was found that when the volume of magnetorheological fluid increased with the addition of 0.1L and 0.3L magnetorheological fluid, the concentricity value decreased, the cylindricity value increased, and the coaxiality increased greatly, reaching 54.5%. The inner cylindricity increased by 42.0%.

Table 3 The results of cylindricity and concentricity test of annular thin-walled parts

MRF volume	+TOL(mm)	MEAS(mm)	DEV(mm)	OUTTOL(mm)	inner cylindricity
Without MRF	0.100	0.013	0.013	0.003	0.01924
With 0.1L MRF	0.100	0.011	0.011	0.002	0.02534
With 0.2L MRF	0.100	0.008	0.008	0.000	0.03018
With 0.3L MRF	0.100	0.005	0.005	0.000	0.03599

From the above data, it can be seen that through adding a suitable volume of magnetorheological fluid, it was possible to provide damping force after excitation solidification. This could improve the stability of the inner hole machining of thin-walled parts and effectively suppress the milling vibration as well as the quality of surface machining.

4. Conclusion

The magnetorheological damping fixture proposed in this paper can effectively suppress the vibration of the workpiece. An improved dynamic response mathematical model of the magnetorheological damping fixture thin-walled parts system of the linear multiple degrees of freedom under forced vibration was established, which provides theoretical and technical basis for the subsequent magnetorheological fluid volumes matching milling quality of workpiece. The results provide a new idea for the use of magnetorheological damping fixtures so as to control the machining quality of thin-walled parts in aerospace. The conclusions are summarized as follows:

1) Through simplifying aerospace thin-walled parts into rectangular thin plates, in accordance with Kirchhoff G.'s small deflection bending theory of elastic thin-plates, Daramberg's principle and the mode superposition principle, an improved dynamic response mathematical model of the magnetorheological damping fixture thin-walled parts system of the linear multiple degrees of freedom, which has different volumes of magnetorheological fluids under forced vibration, was established in this paper. The maximum errors of displacement and acceleration responses of the theoretical calculation value and the experimental value were 16.2% and 15.5%, respectively. The results verified the validity of the model.

2) The dynamics experiment as well as the milling experiment proved that as the increase of the magnetorheological fluid volumes, the natural frequency as well as the damping of the magnetorheological damping fixture-workpiece system increased, and the system's dynamic rigidity and damping characteristics improved. When 5L magnetorheological fluid was added, the vibration abatement was the best.

3) Through comparing the milling quality of thin-walled parts with different volumes of magnetorheological fluids, it was found in this paper that the maximum reduction of roughness was 40%, the coaxiality increased by 54.5%, and the inner cylindricity increased by 42.0%, which effectively and directly verified that through adding a suitable volume of magnetorheological fluid, it was possible to suppress vibration.

Data Availability

The data used to support the findings of this study are included within the article.

Acknowledgements

This project is supported by Shanghai Science and Technology Commission (GrantNo.20ZR1438000).

Contributions

Xiaohui Jiang constructed the idea. Ning Yang performed the experiments and wrote the manuscript, while Yong Zhang and Shan Gao contributed to the conception of the study and helped perform the analysis with constructive discussions.

Corresponding author

Correspondence to Xiaohui Jiang.

Ethical approval

This work does not include human and animal; hence, ethical approval from any committee is not required.

Consent to participate

This work does not include human and animal; hence, ethical approval from any committee is not required.

Consent to publication

The participants have consented to the submission of the case report to the journal.

Conflicts of Interest

The authors declare that they have no conflicts of interest.

Reference

1. Papastathis TN, Ratchev SM, Popov AA (2012) Dynamics model of active fixturing systems for thin-walled parts under moving loads. Int J Adv Manuf Technol 62:1233-1247. https://doi.org/10.1007/s00170-011-3868-3
2. Bakker OJ, Popov AA, Salvi E, Merlo A, Ratchev SM (2011) Model-based control of an active fixture for advanced aerospace components. Proc Inst Mech Eng Part B J Eng Manuf 225:35-51. https://doi.org/10.1177/09544054JEM2042
3. Li Y, Liu C, Hao X, Gao JX, Maropoulos PG (2015) Responsive fixture design using dynamic product inspection and monitoring technologies for the precision machining of large-scale aerospace parts. CIRP Ann - Manuf Technol 64:173-176. https://doi.org/10.1016/j.cirp.2015.04.025
4. Selvakumar S, Arulshri KP, Padmanaban KP, Sasikumar KSK (2013) Design and optimization of machining fixture layout using ANN and DOE. Int J Adv Manuf Technol 65:1573-1586. https://doi.org/10.1007/s00170-012-4281-2
5. Armillotta A, Moroni G, Polini W, Semeraro Q (2010) A unified approach to Kinematic and Tolerance analysis of locating fixtures. Comput Inf Sci Eng 10:1-11. https://doi.org/10.1115/1.3402642
6. Zheng Y, Qian WH (2008) A 3-D modular fixture with enhanced localization accuracy and immobilization capability. Int J Mach Tools Manuf 48:677-687. https://doi.org/10.1016/j.ijmachtools.2007.10.022
7. Wan XJ, Zhang Y (2013) A novel approach to fixture layout optimization on maximizing dynamic machinability. Int J Mach Tools Manuf 70:32-44. https://doi.org/10.1016/j.ijmachtools.2013.03.007
8. Seguy S, Dessein G, Arnaud L (2008) Surface roughness variation of thin wall milling, related to modal interactions. Int J Mach Tools Manuf 48:261-274. https://doi.org/10.1016/j.ijmachtools.2007.09.005
9. Meshreki M, Attia H, Kövecses J (2011) Development of a new model for the varying dynamics of flexible pocket-structures during machining. J Manuf Sci Eng Trans ASME 133. https://doi.org/10.1115/1.4004322
10. Li X, Zhao W, Li L, He N, Chi S (2015) Modeling and application of process damping in milling of thin-walled workpiece made of titanium alloy. Shock Vib 2015. https://doi.org/10.1155/2015/431476

11. Zhou X, Zhang D, Luo M, Wu B (2014) Toolpath dependent chatter suppression in multi-axis milling of hollow fan blades with ball-end cutter. Int J Adv Manuf Technol 72:643-651. https://doi.org/10.1007/s00170-014-5698-6
12. Liu Y, Zhang D, Wu B. (2012) An efficient full-discretization method for prediction of milling stability. Int J Mach Tools Manuf 63:44-48. https://doi.org/10.1016/j.ijmachtools.2012.07.008
13. Lv S, Zhao Y (2021) Stability of Milling Process with Variable Spindle Speed Using Runge–Kutta-Based Complete Method. Math Probl Eng 2021:1-10. https://doi.org/10.1155/2021/6672513
14. Luo M, Zhang DH, Wu BH, Zhou X (2011) Material removal process optimization for milling of flexible workpiece considering machining stability. Proc Inst Mech Eng Part B J Eng Manuf 225:1263-1272. https://doi.org/10.1177/2041297510393650
15. Wan XJ, Zhang Y, Huang XD (2013) Investigation of influence of fixture layout on dynamic response of thin-wall multi-framed work-piece in machining. Int J Mach Tools Manuf 75:87-99. https://doi.org/10.1016/j.ijmachtools.2013.09.008
16. Zeng S, Wan X, Li W, Yin Z, Xiong Y (2012) A novel approach to fixture design on suppressing machining vibration of flexible workpiece. Int J Mach Tools Manuf 58:29-43. https://doi.org/10.1016/j.ijmachtools.2012.02.008
17. Wang Y, Chen X, Gindy N, Xie J (2008) Elastic deformation of a fixture and turbine blades system based on finite element analysis. Int J Adv Manuf Technol 36:296-304. https://doi.org/10.1007/s00170-006-0841-7
18. Meshreki M, Kövecses J, Attia H, Tounsi N (2008) Dynamics modeling and analysis of thin-walled aerospace structures for fixture design in multiaxis milling. J Manuf Sci Eng Trans ASME 130:0310111-03101112. https://doi.org/10.1115/1.2927444
19. Dong Z, Jiao L, Wang X, Liang Z, Liu Z, Yi J (2016) FEA-based prediction of machined surface errors for dynamic fixture-workpiece system during milling process. Int J Adv Manuf Technol 85:299-315. https://doi.org/10.1007/s00170-015-7854-z
20. Rai JK, Xirouchakis P (2008) Finite element method based machining simulation environment for analyzing part errors induced during milling of thin-walled components. Int J Mach Tools Manuf 48:629-643. https://doi.org/10.1016/j.ijmachtools.2007.11.004
21. Yang Y, Xu D, Liu Q (2015) Vibration Suppression of Thin-Walled Workpiece Machining Based on Electromagnetic Induction. Mater Manuf Process 30:829-835. https://doi.org/10.1080/10426914.2014.962042
22. Pour DS, Behbahani S (2016) Semi-active fuzzy control of machine tool chatter vibration using smart MR dampers. Int J Adv Manuf Technol 83:421-428. https://doi.org/10.1007/s00170-015-7503-6
23. Yang Y, Xu D, Liu Q (2015) Milling vibration attenuation by eddy current damping. Int J Adv Manuf Technol 81:445-454. https://doi.org/10.1007/s00170-015-7239-3
24. Ma J, Zhang D, Wu B, Luo M, Chen B (2016) Vibration suppression of thin-walled workpiece machining considering external damping properties based on magnetorheological fluids flexible fixture. Chinese J Aeronaut 29:1074-1083. https://doi.org/10.1016/j.cja.2016.04.017
25. Ma J, Zhang D, Wu B, Luo M, Liu Y (2017) Stability improvement and vibration suppression of the thin-walled workpiece in milling process via magnetorheological fluid

flexible fixture. Int J Adv Manuf Technol 88:1231-1242. https://doi.org/10.1007/s00170-016-8833-8

26. Bae JS, Park JS, Hwang JH, Roh JH, Pyeon B Do, Kim JH (2018) Vibration Suppression of a Cantilever Plate Using Magnetically Multimode Tuned Mass Dampers. Shock Vib 2018. https://doi.org/10.1155/2018/3463528
27. Xin DK, Nie SL, Ji H, Yin FL (2018) Characteristics, Optimal Design, and Performance Analyses of MRF Damper. Shock Vib 2018. https://doi.org/10.1155/2018/6454932

Figures

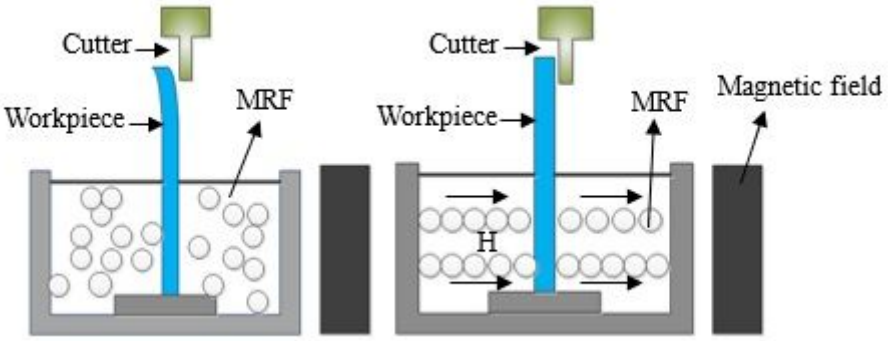

Figure 1

The magnetorheological fluid in the magnetorheological fixture is magnetically solidified.

Figure 2

Aerospace thin-walled parts

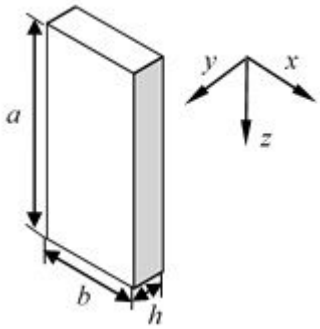

Figure 3

Simplified rectangular thin-walled plate

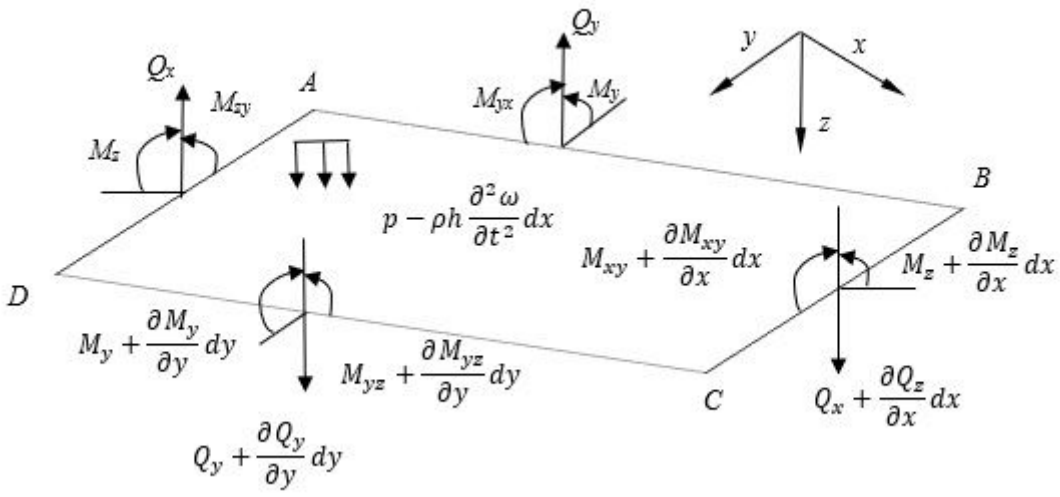

Figure 4

The rectangular micro-element body on the neutral surface of the rectangular thin-walled plate

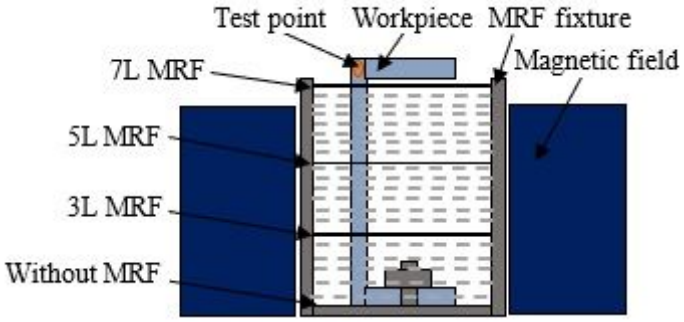

Figure 5

Fixtures with different volumes of magnetorheological fluid

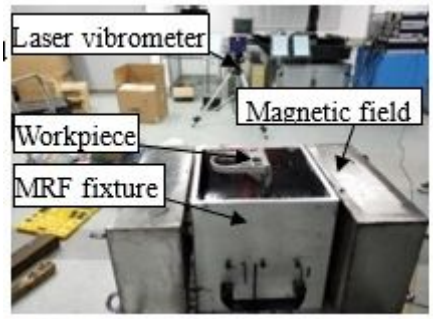

Figure 6

Modal percussion experiment

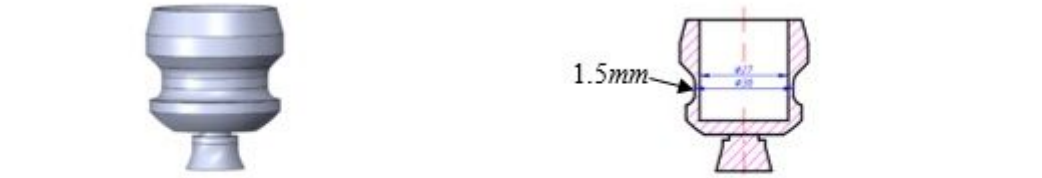

(a) Three-dimensional drawing of annular thin-walled parts (b) The dimensions of annular thin-walled part

Figure 7

Schematic diagram of ring-shaped thin-walled parts

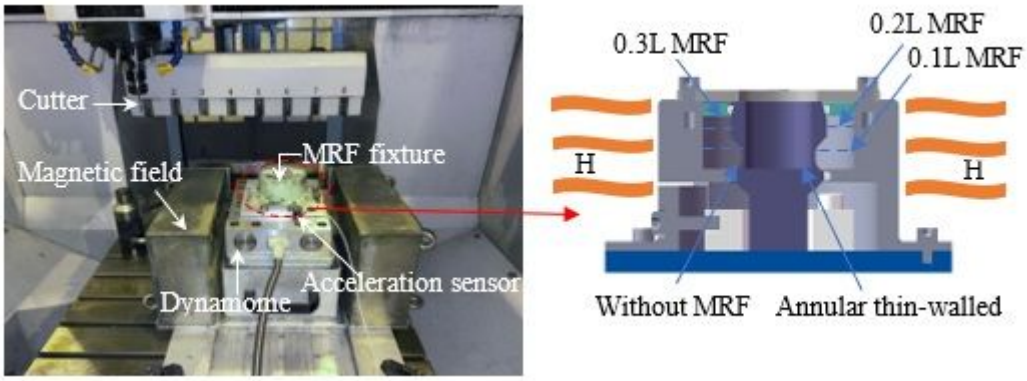

Figure 8

Measurement of milling force and vibration acceleration

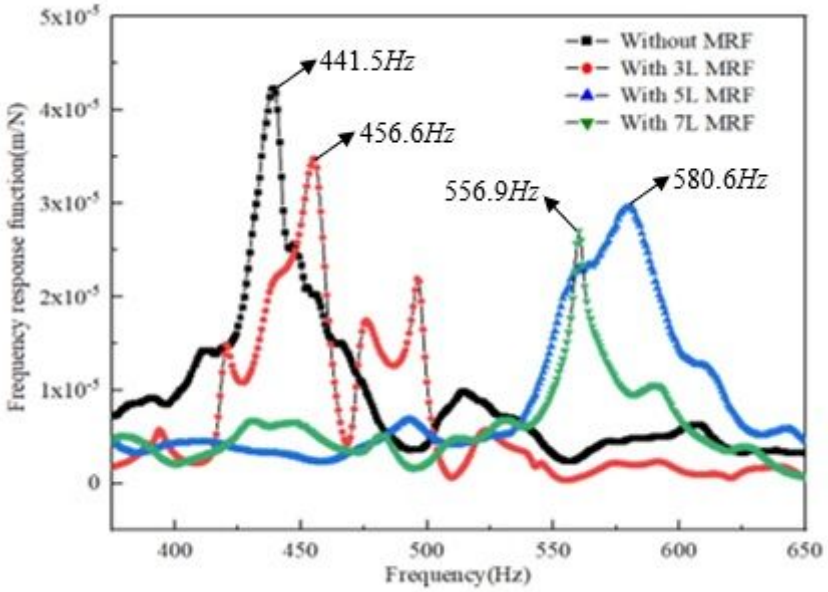

Figure 9

The frequency response function with different magnetorheological fluid volumes added

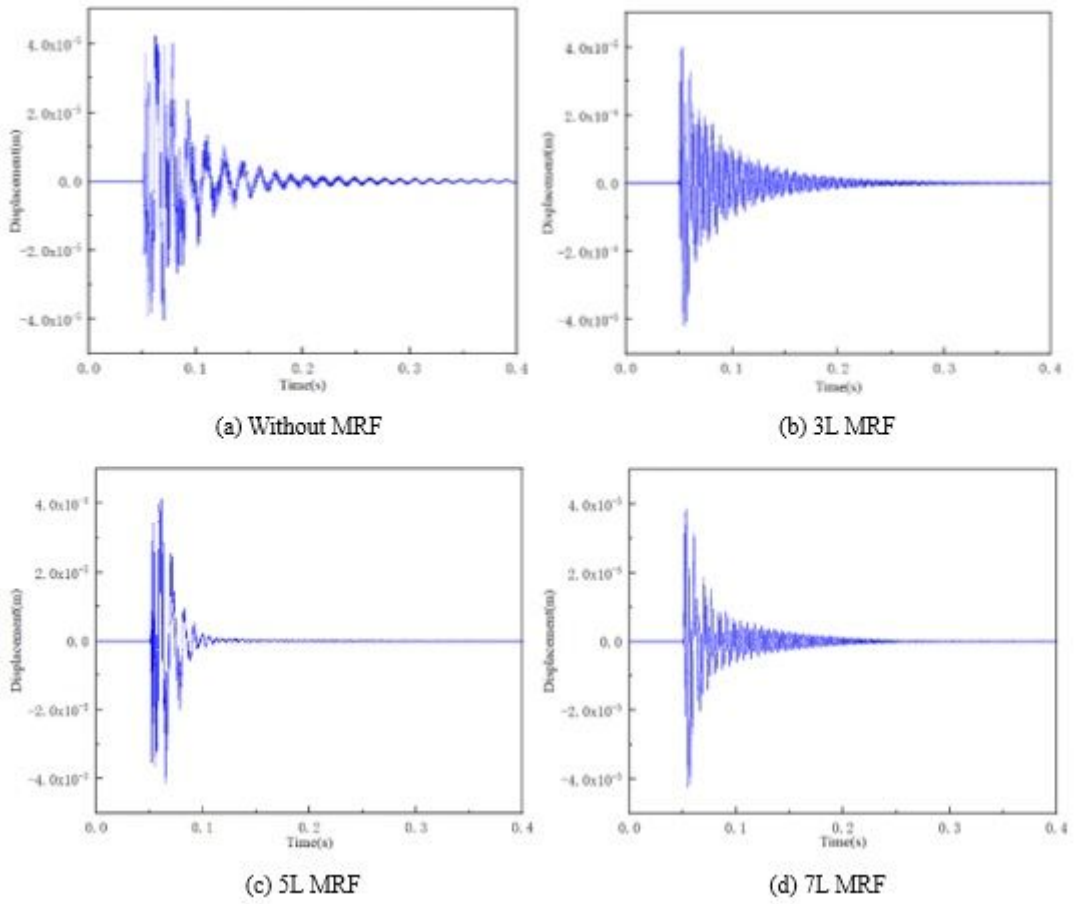

Figure 10

The displacement response with different magnetorheological fluid volumes added

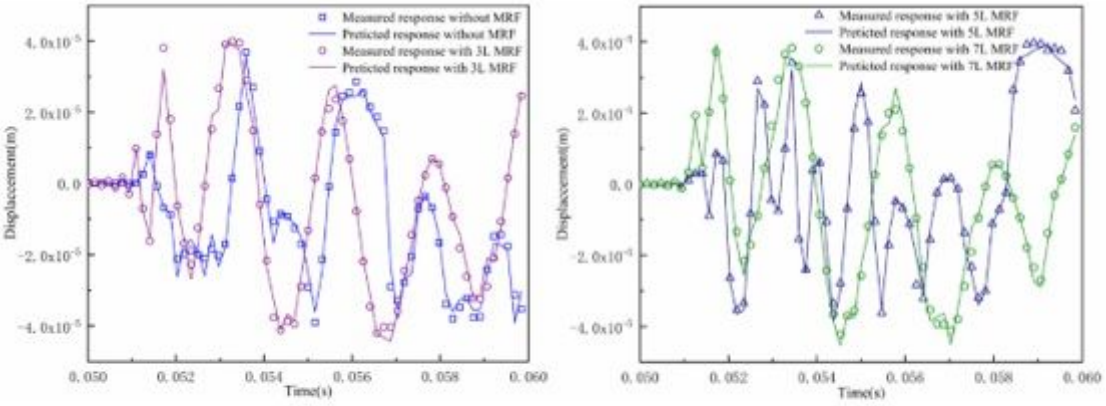

Figure 11

Comparison of the predicted and measured displacement response with different magnetorheological fluid volumes

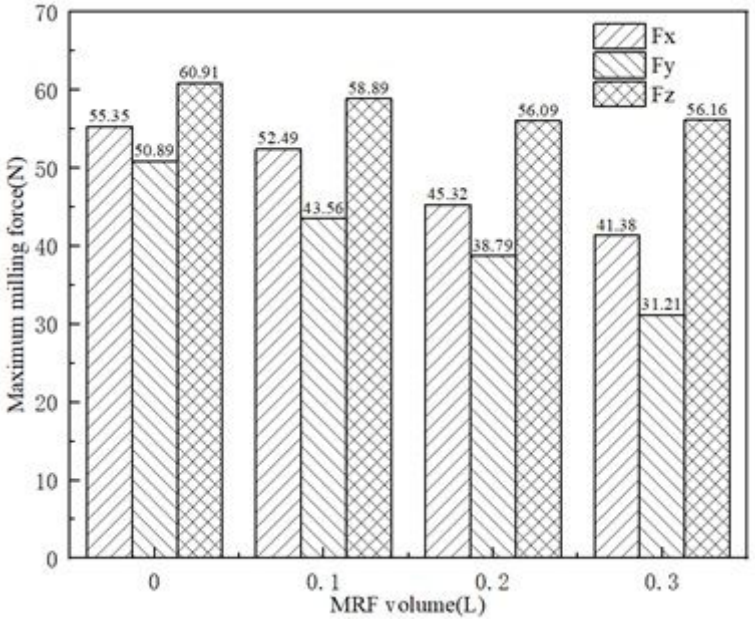

Figure 12

The maximum milling force with different volumes of magnetorheological fluids

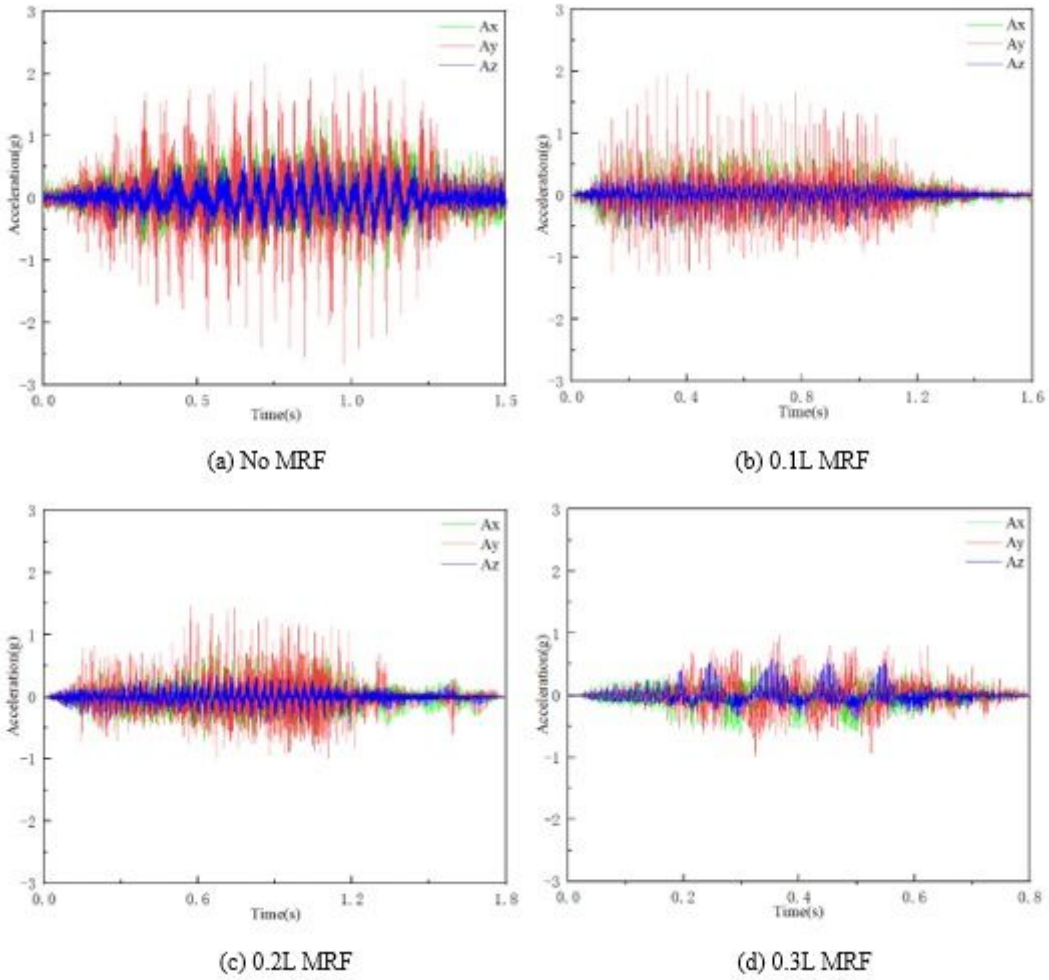

Figure 13

The milling vibration acceleration with different volumes of magnetorheological fluids

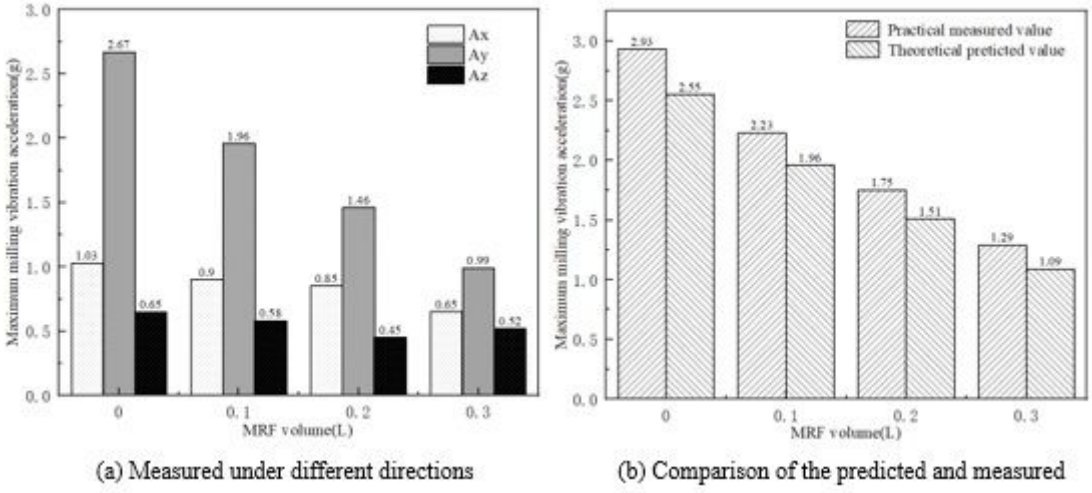

(a) Measured under different directions (b) Comparison of the predicted and measured

Figure 14

Maximum vibration acceleration with different volumes of magnetorheological fluids

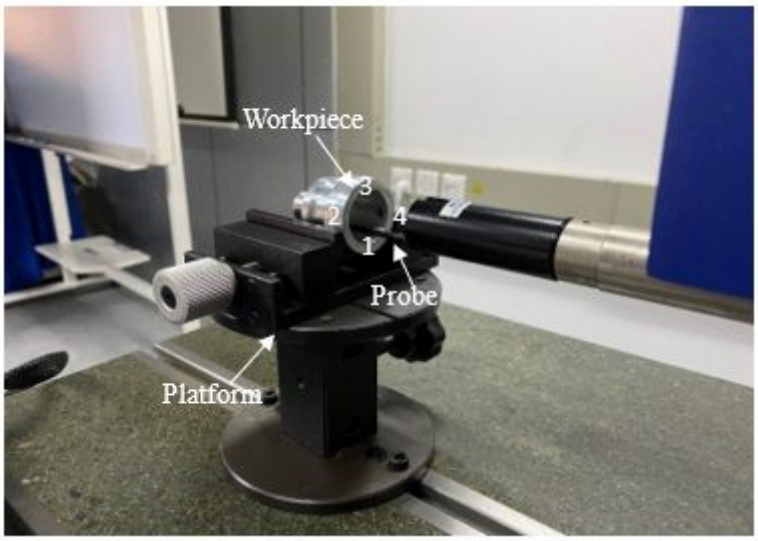

Figure 15

Scheme of roughness measurement

(a) Scheme of Cylindricity measurement (b) Scheme of Coaxiality measurement

Figure 16

Scheme of cylindricity and concentricity measurement